# Energy Beamforming for Cooperative Localization in Wireless-Powered Communication Network

Yubin Zhao, *Member, IEEE*, Xiaofan Li, *Senior Member, IEEE*, Huaming Wu, *Member, IEEE*, and Cheng-Zhong Xu, *Fellow, IEEE*

***Abstract*—Two functions are essential and necessary for the wireless-powered communication network, which are energy beamforming and localization. On one hand, energy beamforming controls the wireless energy waves of the energy access point (E-AP) in order to activate the nodes for transmitting information. On the other hand, locating the nodes is important to network management and location-based services in the wireless power communication network (WPCN). For a large-scale network, cooperative localization that employs neighborhood nodes to participate in positioning unknown target nodes is highly accurate and efficient. However, how to use energy beamforming to achieve highly accurate localization is not fully investigated yet. In this article, we analyze the impacts of energy beamforming on the cooperative localization performance of WPCNs. We formulate the Fisher information matrix (FIM) and the corresponding Cramér–Rao lower bound (CRLB) for the full connected network and a single node, respectively. Then, we propose beamforming schemes to optimize the cooperative localization and the power consumption. For optimal localization problems, we derive the closed-form expression of the optimal energy beamforming. For the optimal energy efficiency problems, we propose semidefinite programming (SDP) solutions to achieve the minimum power consumption while using calibrations to approach the actual localization requirements. Further, we also analyze the impacts of channel uncertainty. Through extensive simulations, the results demonstrate the dominant factors of the localization performance, and the performance improvements of our proposed schemes, which outperform the existing power allocation schemes.**

***Index Terms*—Cooperative localization, energy efficiency, Fisher information matrix (FIM), semidefinite programming (SDP), wireless power transfer.**

## I. Introduction

In THE recent years, radio-frequency (RF) power transfer has become an effective alternative technique to supply continuous energy for the remote next-generation wireless networks [1]. The conventional energy-constrained wireless networks have a limited lifetime, which consume lots of efforts to maintain the batteries, such as wireless sensor networks. In contrast, the wireless network equipped with an RF energy harvesting module has a sustainable power supply from the radio environment. Consequently, with the appearance of the commercialized products, e.g., Powercast, wireless power communication networks (WPCNs) have drawn much attention [2]. As a promising network of future IoT systems, the architecture, waveform design, beamforming, and network optimization are extensively investigated.

Compared with wireless communication networks (WCNs) [3], WPCNs show advantages in lifetime and cost. The lifetime of WPCN can be extended as long as possible with a single energy access point (E-AP). Because such E-AP can provide continuous wireless energy for the passive nodes, the lifetime of WCN is limited by the batteries equipped in the nodes. No matter what kind of energy efficient strategies are used, the batteries will be depleted finally. Even if all the nodes are connected with the power lines, the mobility is limited and the costs are increased. In addition, the cost of each node in WPCN is much lower than WCN, since no battery is required and the architecture of the chip is much simpler. In this case, a large-scale network can be constructed.

Similar to other wireless networks, WPCNs contain a large number of deployed nodes sensing, gathering, and communicating information with other nodes [4]. Therefore, the knowledge of node positions is becoming important for network management and optimization strategies. On the other hand, positioning the nodes in WPCNs also provides cost-effective location-based services. However, using GPS is not only an expensive solution but infeasible in some harsh environments, e.g., in buildings, in urban canyons, under tree canopies, or in caves. Thus, a fast, cost-effective, and high-accurate localization technique is required for large-scale WPCNs.

Manuscript received December 11, 2020; revised February 17, 2021; accepted March 18, 2021. Date of publication March 23, 2021; date of current version August 24, 2021. This work was supported in part by National Key Research and Development Program of China under Grant 2019YFB2102100; in part by the National Nature Science Foundation of China under Grant 61801306; in part by the Shenzhen Fundamental Research under Grant JCYJ20180302145755311; in part by the Guangdong Special Fund for Science and Technology Development under Grant 2019A050503001; and in part by the Science and Technology Development Fund of Macao SAR (FDCT) under Grant 0015/2019/AKP. *(Corresponding author: Xiaofan Li.)*

Yubin Zhao is with the School of Microelectronics Science and Technology, Sun Yat-sen University, Zhuhai 519082, China (e-mail: zhaoyb23@mail.sysu.edu.cn).

Xiaofan Li is with the School of Intelligent System Science and Engineering, Jinan Unniversity, Zhuhai 519070, China (e-mail: lixiaofan@jnu.edu.cn).

Huaming Wu is with the Center for Applied Mathematics, Tianjin University, Tianjin 300072, China (e-mail: whming@tju.edu.cn).

Cheng-Zhong Xu is with the State Key Laboratory of IoTSC, Department of Computer and Information Science, University of Macau, Macau, China (e-mail: czxu@um.edu.mo).

Digital Object Identifier 10.1109/JIOT.2021.3068284

Cooperative localization employs nodes exchange radio signals to attain the range measurements [5]. Such technique offers additional localization accuracy gain by enabling the neighbor nodes to help each other in estimating positions, which is suitable for WPCNs in a high density and large-scale deployment scenario. In cooperative localizations, nodes with known positions are called anchors, which are sparsely deployed and used to locate other nodes. The nodes with unknown positions are called targets. In WPCN, all nodes including anchors and targets are batteryless and powered up by the E-APs, which are either centralized deployed with MIMO antennas or distributed deployed throughout the playing field. The ranging measurements of cooperative localization can be attained only as if the nodes gain enough energy from E-APs. Thus, the microwave propagations in cooperative localization-based WPCN consist of energy beamforming of E-AP and the ranging measurements. The energy beamforming directly influences the ranging and the localization accuracy [6], [7]. Using the cooperative localization technique, the WPCN has two kinds of potential applications. On one hand, WPCN can track nodes widely deployed in the environment without considering the battery depletion, e.g., the sensor tags in the manufactory, hospital, and tunnel [8], [9]. In addition, the UAVs are potential mobile wireless power transfer devices for such an application [10]. On the other hand, such a system can be used as the indoor localization for large-scale shop malls or factories, since the batteryless nodes can be designed as anchors, which are activated by the wireless power. Such devices are small and the cost is even small than other indoor localization systems, e.g., iBeacon [11].

To analyze the impact of energy beamforming on localization performance in this article, the Fisher information matrix (FIM) is utilized as the fundamental tool and squared position error bound (SPEB) is introduced as the major metric for evaluation, which are widely applied in many researches [12]–[14]. Within the FIM framework, the beamed wireless power signal, channel information, network topology are fully analyzed, and the optimization objectives are constructed. Then, wireless power beamforming strategies can be developed to minimize the position estimation errors or the energy consumption.

Our major contributions are as follows: first, we formulate the FIM of full-connected WPCN within a cooperative framework, which fully considers the energy beamforming, network topology, signal noise, and cooperative ranging measurements. The impacts of beamforming waves on the localization performance in E-APs are clearly illustrated in the form of the FIM. Then, the second contribution is that we introduce the beamforming schemes to solve two optimization problems, which are: 1) the minimization of position estimation error with transmitted power constraints and 2) the minimization of energy consumption problem with node localization requirements. We prove that the SPEBs in the objectives are bounded by the inverse forms of the FIM trace, in which the objectives are turned into quadratically constrained quadratic programmings (QCQPs). Then, the optimization problems are efficiently solved by obtaining the close form expression or using semidefinite programming (SDP). Third, the spatial recursive FIM formulations and optimization strategies for a single node are exploited with the prior information of other nodes. We derive the upper bound of spatial recursive FIM to develop simplified beamforming solutions. To overcome the over relaxation problems, we employ a calibration method for the SDP solutions. The final contribution is that we analyze the impacts of channel estimation error on localization estimation performances.

Our analysis and proposed beamforming schemes are evaluated in extensive simulations. We compare our schemes with SDP-based power allocation solutions and equally combing method. Then, the impacts considering the channel uncertainty are also presented. The results demonstrate that our schemes can greatly improve the estimation accuracy and reduce the minimum energy consumption with a given localization requirement.

The remainder of this article is organized as follows: Section II presents the related works of the WPCN and cooperative localization; Section III provides the system model and the FIM formulations; the beamforming schemes for full connected network are introduced in Section IV and the optimizations for single node are presented in Section V; Section VI formulates the impacts of channel uncertainty; the simulations are presented in Sections VII and VIII concludes the whole paper.

## II. Related Work

WPCN has gain much attention since it is first introduced in [15] and [16]. Then, many researches utilize various techniques to improve the data transmission quality or reliability, e.g., beamforming strategies [17], [18], network design [19], [20], MAC control schemes [21], [22], and cooperative strategies [23], [24]. Considering 3-D space, UAVs are employed as the wireless power transfer base stations, and the related joint resource allocation and trajectory plan are investigated [10], [25]. Recently, some passive devices in WPCN are designed to provide localization services, e.g., using backscatter communications [26] or converting the harvested energy into UWB signals [27]. Pannuto *et al.* [28] proposed a UWB-based backscatter device, which can achieve 30-cm localization accuracy. Fantuzzi *et al.* [29]–[31] proposed circuit designs to convert the UHF microwave into UWB signals and provide TDOA ranging.

In addition to hardware design, communication strategies and localization methods in WPCNs are also exploited, especially in WSN area. El Assaf *et al.* [32] proposed a hop count method to estimate the node positions in energy harvested WSN. Chang *et al.* [33] introduced a passive WSN, in which the node was activated by the RF power, and angle division and grid division methods were developed with adapting the RF propagation directions to derive the node positions. Belo *et al.* [34] used an antenna arrays to estimate single-node location based on RSS value. Aziz *et al.* [35] introduced a batteryless IoT node with two antennas, and employed 64 antenna array to simultaneously provide wireless power and track the node. In [36], the batteryless anchors are introduced and power allocation schemes for single target tracking are proposed to improve the system performance. Although some localization algorithms are investigated in WPCN, these methods are

only applicable for single node or target, which is difficult to implement in the large-scale network.

In wireless cooperative localization research, lots of theoretical investigations and localization algorithms appear in the recent years [37]. In general, the cooperative localization is an efficient method of the self-organized large-scale network to manage the network and tracking multiple targets. However, the localization error can also propagate throughout the whole network when the target nodes contain localization errors and help locate the new joined node. Shen *et al.* [38] derived the equivalent FIM (EFIM) of cooperative localization and used SPEB as the main metric to evaluate the positioning accuracy. This work demonstrated that lots of targets provide ranging information when only a few anchors are deployed in a large-scale network. Then, the localization accuracy is increased with such information. However, analyzing the fundamental performance of cooperative localization is complex. Consequently, resource allocations are also complex and the distributed strategies may only converge to local optimal values. Thus, the power control and bandwidth allocation schemes using SDP, gaming, and machine learning methods for wideband systems are exploited [39]–[42]. For cooperative localization algorithms, distributed localization algorithm outperforms the centralized algorithm in cooperative localization since the data flow from targets and anchors are reduced. In this case, the operation expense of cooperative localization is much lower than the conventional localization. A linear distributed algorithm framework is introduced in [43]. Nguyen *et al.* [44] proposed a least squared method in the cooperative localization. Furthermore, SDP for relaxing the least squared method was also proposed in [45]. Note that, compared with WCNs, the localization accuracy of WPCN is lower with the same number of nodes. Because, the power transfer efficiency of WPCN is quite low, which leads to the low accuracy estimation. In addition, the nodes of WPCN are also low power chips, which means that the nodes can only provide single frequency carrier RSS value for ranging. However, nodes in WCN are active, which can provide wideband singles for localization, e.g., CSI values. In this case, the accuracy is much higher than WPCN. However, the theoretical foundations and optimizations for cooperative localization in WPCNs are not fully investigated yet.

## III. System Model

The WPCN consists of E-AP and the wireless communication nodes, which is illustrated in Fig. 1. The nodes with perfect knowledge of their positions are defined as anchors, and the nodes without their position knowledge are defined as targets. All the nodes are equipped without batteries. We use $N_A$ and $N_T$ to denote the number of anchors and targets, respectively. The set of anchors is denoted by $\mathcal{N}_A = \{1, 2, \ldots, N_A\}$ and the set of targets is denoted by $\mathcal{N}_T = \{1, 2, \ldots, N_T\}$. The position of anchor $j$ is denoted by $\mathbf{a}_j \triangleq [a_j^X, a_j^Y]^T$, and the position of target $i$ is denoted by $\mathbf{p}_i \triangleq [p_i^X, p_i^Y]^T$.

The E-AP contains multiple antennas and provides the wireless power beam to turn on the batteryless nodes. We use $K$ to denote the number of antennas in E-AP. Let $\mathbf{G} \triangleq [\mathbf{g}_1, \mathbf{g}_2, \ldots, \mathbf{g}_N]^T$ be the downlink wireless power channel matrix from the E-AP to the nodes, and define $g_{kn} \triangleq [\mathbf{G}]_{kn}$ as the channel coefficient between the $k$th antenna of the E-AP and the node $n$. To distinguish the wireless power beam channel to the anchors and the cooperative nodes, we define $\mathbf{G}_A$ as the anchor channel matrix, which indicate the channel from E-AP to the anchors, and define $\mathbf{G}_C$ as the target channel matrix to indicate the channel from E-AP to the target nodes. Let $d_{ji} = ||\mathbf{a}_j - \mathbf{p}_i||$ be the range (or distance) between anchor $j$ and target $i$. Similarly, let $d_{im} = ||\mathbf{p}_i - \mathbf{p}_m||$ be the range between target $i$ and $m$, where $i \neq m$. The anchors will send ranging signals to the targets when attaining sufficient energy, and the targets also send the ranging signals to each other to form a fully connected network and cooperatively locate themselves.

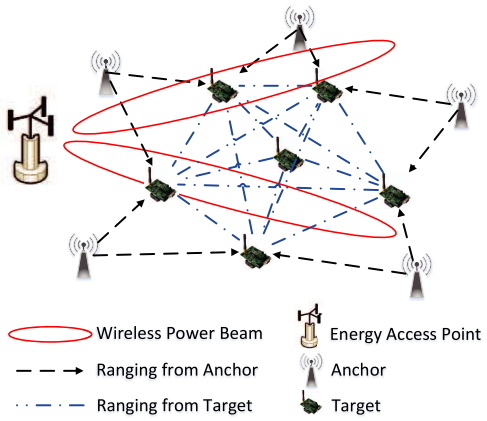


Fig. 1. Architecture of WPCLoc.

### A. Wireless Power Transfer Phase

The E-AP generates a signal vector $\boldsymbol{x} = [x_1, x_2, \ldots, x_K]^T$ to form a wireless power beam. The anchors are activated by such signals. On the network node side, the received signal for node $n$ is

$$y_n = \mathbf{g}_n \boldsymbol{x} + v_0^n = \sum_{k=1}^{K} g_{kn} x_k + v_0^n \tag{1}$$

where $n \in \mathcal{N}_A \bigcup \mathcal{N}_T$ and $v_0^n$ is the additive noise which follows zero-mean Gaussian distribution. For the wireless power beam, we assume that the received energy is mainly from the E-AP, and $v_0^n$ is too small to power up the device, which cannot be collected as the energy source. Then, the received power $r_y^n = \mathbb{E}_{y_n}(||y_n||^2)$ of node $n$ is

$$r_y^n = \mathbb{E}_{\boldsymbol{x}}\left(\boldsymbol{x}^T \mathbf{g}_n^T \mathbf{g}_n \boldsymbol{x}\right). \tag{2}$$

### B. Cooperative Range Measurement Phase

After obtaining the energy from E-AP, network nodes, including anchors and targets, will encode the ranging data and forward to the other nodes. When node $n$ sends the ranging signal to target $i$, the received signal is

$$z_{ni} = h_{n,i}\left(d_{n,i}\right) y_n + v_e^{ni} \tag{3}$$

where $n \neq i$, $h_{n,i}(\cdot)$ is the channel response of $y_n$ which considers the path loss according to the range $d_{n,i} = ||\boldsymbol{p}_n - \boldsymbol{p}_i||$ between node $n$ and $i$. Take a flat fading propagation channel for instance, we have $h_{ni}(d_{n,i}) = (f_c/[4\pi d_{n,i}])^{\beta}\sqrt{\xi_{n,i}}$ where $f_c$ is the central frequency of the signal, $\beta$ is the fading factor, and $\xi_{n,i}$ is the channel gain.

### C. Fisher Information Matrix

To derive the fundamental performance, we employ FIM as the analysis tool. First, we define $\boldsymbol{\theta}$ as the vector of the unknown target position states

$$\boldsymbol{\theta} = \left[\mathbf{p}_1^T \ \mathbf{p}_2^T \ \cdots \ \mathbf{p}_{N_T}^T\right]^T. \tag{4}$$

Then, we define $\boldsymbol{z}$ as the observation vector of all the received signals on the target side

$$\boldsymbol{z} = \left[\boldsymbol{z}_A^T \ \boldsymbol{z}_C^T\right]^T \tag{5}$$

where $\boldsymbol{z}_A$ and $\boldsymbol{z}_C$ indicate the observations from anchors and cooperative targets, respectively

$$\begin{cases} \boldsymbol{z}_A = \left[\boldsymbol{z}_1^{A^T} \ \boldsymbol{z}_2^{A^T} \ \cdots \ \boldsymbol{z}_i^{A^T} \ \cdots \ \boldsymbol{z}_{N_T}^{A\ T}\right]^T \\ \boldsymbol{z}_C = \left[\boldsymbol{z}_1^{C^T} \ \boldsymbol{z}_2^{C^T} \ \cdots \ \boldsymbol{z}_i^{C^T} \ \cdots \ \boldsymbol{z}_{N_T}^{C\ T}\right]^T \end{cases} \tag{6}$$

and $\boldsymbol{z}_i^A$ and $\boldsymbol{z}_i^C$ indicate the received signal vectors of target $i$ from anchors and targets, respectively

$$\begin{cases} \boldsymbol{z}_i^A = \left[z_{1i} \ z_{2i} \ \cdots \ z_{ji} \ \cdots \ z_{N_A i}\right]^T \\ \boldsymbol{z}_i^C = \left[z_{1i} \ z_{2i} \ \cdots \ z_{mi} \ \cdots \ z_{N_T i}\right]^T \end{cases} \tag{7}$$

where $m \in \mathcal{N}_T$. Here, we define $z_{ii} = 0, i \in \mathcal{N}_T$ for future calculation. The joint probability distribution $f(\boldsymbol{\theta}, \boldsymbol{z}) = f(\boldsymbol{z}|\boldsymbol{\theta})f(\boldsymbol{\theta})$, where $f(\boldsymbol{z}|\boldsymbol{\theta})$ is the likelihood function, and $f(\boldsymbol{\theta})$ is the prior distribution of $\boldsymbol{\theta}$. $f(\boldsymbol{z}|\boldsymbol{\theta})$ can be expressed as

$$f(\boldsymbol{z}|\boldsymbol{\theta}) = \prod_{i=1}^{N_T}\left(\prod_{m=1}^{N_T} f\left(z_{mi}|\boldsymbol{p}_i\right)\prod_{j=1}^{N_A} f\left(z_{ji}|\boldsymbol{p}_i\right)\right) \tag{8}$$

where we define $f(z_{ji}|\boldsymbol{p}_i) = 1, i \in \mathcal{N}_T$.

Next, we define $\widetilde{\boldsymbol{\theta}}$ as the unbiased estimator of $\boldsymbol{\theta}$ based on $\boldsymbol{z}$. The Cramér–Rao lower bound (CRLB) indicates that the covariance of $\widetilde{\boldsymbol{\theta}}$ should satisfy the information inequality

$$\mathbb{E}_{z,\boldsymbol{\theta}}\left\{\left(\widetilde{\boldsymbol{\theta}} - \boldsymbol{\theta}\right)\left(\widetilde{\boldsymbol{\theta}} - \boldsymbol{\theta}\right)^T\right\} \succeq \mathbf{J}_{\boldsymbol{\theta}}^{-1} \tag{9}$$

where $\mathbf{J}_{\boldsymbol{\theta}}$ is the FIM for $\boldsymbol{\theta}$ given by

$$\mathbf{J}_{\boldsymbol{\theta}} = \mathbb{E}_{z,\boldsymbol{\theta}}\left\{\nabla_{\boldsymbol{\theta}} \ln f(\boldsymbol{\theta}, \boldsymbol{z})\left[\nabla_{\boldsymbol{\theta}} \ln f(\boldsymbol{\theta}, \boldsymbol{z})\right]^T\right\} \tag{10}$$

where $\nabla_{\boldsymbol{\theta}}$ is the first-order partial derivatives operator of $\boldsymbol{\theta}$. Then, we have the following proposition.

*Proposition 1:* The FIM of all the target nodes in WPCN is given by (12), shown at the bottom of the page, where $\mathbf{J}_{\boldsymbol{\theta}}$ is a $2N_T \times 2N_T$ matrix. $\mathbf{J}_A(\boldsymbol{p}_i)$ and $\mathbf{C}_{i,m}$ are expressed as follows:

$$\begin{cases} \mathbf{J}_A(\boldsymbol{p}_i) = \sum_{j=1}^{N_A} \lambda_{j,i}\mathbf{J}(\phi_{j,i}) & j \in \mathcal{N}_A \\ \mathbf{C}_{m,i} = \left(\lambda_{i,m} + \lambda_{m,i}\right)\mathbf{J}(\phi_{m,i}) & i, m \in \mathcal{N}_T \end{cases} \tag{11}$$

where $\lambda_{m,i}$ is derived based on (47); $\mathbf{J}(\phi_{m,i}) = \mathbf{q}_{m,i}\mathbf{q}_{m,i}^T$ is the angle-of-arrival (AOA) matrix, $\mathbf{q}_{m,i} = [\cos\phi_{m,i} \ \sin\phi_{m,i}]^T$ with $\phi_{m,i} = \arctan[(p_i^X - p_m^X)/(p_i^Y - p_m^Y)]$ denoting the AOA from node $m$ to node $i$.

*Proof:* Refer to Appendix A for the detailed derivation. ■

Note that this FIM formulation is constructed based on the framework of cooperative localization [38]. Proposition 1 illustrates the relationship between the wireless power transfer and the localization accuracy and provides the new model of equivalent ranging coefficient (ERC) within the FIM framework. Specifically, $\lambda_{i,m}$ and $\lambda_{j,i}$ are reformulated compared with [38], where $\lambda_{i,m}$ is formulated as

$$\lambda_{i,m} = r_y^m \frac{\xi_{i,m}\beta^2\left(\frac{f_c}{4\pi}\right)^{2\beta}}{d_{i,m}^{2\beta+2}N_0} \tag{13}$$

in which $r_y^m$ is determined by the wireless node since the node is active. However, $r_y^m$ in this article is attained by wireless power transfer, which is $r_y^m = \mathbb{E}_{\boldsymbol{x}}(\boldsymbol{x}^T\mathbf{g}_m^T\mathbf{g}_m\boldsymbol{x})$. Then, we have

$$\lambda_{i,m} = \mathbb{E}_{\boldsymbol{x}}\left(\boldsymbol{x}^T\mathbf{g}_m^T\mathbf{g}_m\boldsymbol{x}\right)\frac{\xi_{i,m}\beta^2\left(\frac{f_c}{4\pi}\right)^{2\beta}}{d_{i,m}^{2\beta+2}N_0}. \tag{14}$$

It is clearly observed that $\boldsymbol{x}$ is the beamforming strategy and $\boldsymbol{x}^T\mathbf{g}_m^T\mathbf{g}_m\boldsymbol{x}$ determines the localization accuracy directly in (12). Thus, the two phase propagations are integrated as a new FIM. For instance, $\lambda_{i,m} = \lambda_{m,i}$ for WCNs if both active nodes send the same signal powers. However, in our system, $\lambda_{i,m} \neq \lambda_{m,i}$ even if $\boldsymbol{x}$ contains the same waveforms for all the antennas. Because the wireless power propagation channels from antennas to the nodes are different.

### D. Squared Position Error Bound

Although CRLB is the widely used localization performance indicator for unbiased estimation algorithms, a specified scalar value is preferred to quantify the localization accuracy. Generally, the mean square error (MSE) or root mean squared error (RMSE) are closely related to the trace of CRLB. In this case, SPEB which is the trace of CRLB is employed as the optimal performance metric [3]. For a single target node, we define SPEB as

$$\mathcal{P}\left(\boldsymbol{p}_i\right) \triangleq \mathrm{tr}\left\{\mathbf{J}^{-1}\left(\boldsymbol{p}_i\right)\right\}. \tag{15}$$

$$\mathbf{J}(\boldsymbol{\theta}) = \begin{pmatrix} \mathbf{J}_A(\boldsymbol{p}_1) + \sum_{m\neq 1}\mathbf{C}_{1,m} & -\mathbf{C}_{1,2} & \cdots & -\mathbf{C}_{1,N_T} \\ -\mathbf{C}_{1,2} & \mathbf{J}_A(\boldsymbol{p}_2) + \sum_{m\neq 2}\mathbf{C}_{2,m} & \cdots & -\mathbf{C}_{2,N_T} \\ \vdots & \vdots & \ddots & \vdots \\ -\mathbf{C}_{1,N_T} & -\mathbf{C}_{2,N_T} & \cdots & \mathbf{J}_A(\boldsymbol{p}_{N_T}) + \sum_{m\neq N_T}\mathbf{C}_{N_T,m} \end{pmatrix} \tag{12}$$

Then, for multiple target nodes, the SPEB is expressed as follows:

$$\mathcal{P}(\boldsymbol{\theta}) \triangleq \sum_{i=1}^{N_T} \mathrm{tr}\Big\{\mathbf{J}^{-1}\big(\boldsymbol{p}_i\big)\Big\} = \mathrm{tr}\Big\{\mathbf{J}^{-1}(\boldsymbol{\theta})\Big\}. \tag{16}$$

In addition, using SPEB as the scalar value can derive a tighter bound during relaxing the following optimization problems.

## IV. Beamforming Schemes for Full Connected Network

### A. Localization Accuracy Optimization

It is clearly observed that the wireless power beam directly influence the localization performance. With the given FIM to indicate the SPEB, we formulate beamforming problems for WPCNs as the optimal cooperative localization problem.

Considering the sum of transmitter power is constrained, the minimum SPEB is to decide how to design the wireless power wave forms to achieve the minimum location estimation error

$$\begin{aligned}(\mathbb{P}_1):\ &\min_{\boldsymbol{x}}\ \mathcal{P}(\boldsymbol{\theta})\\ &\text{s.t.}\ \ \mathbb{E}_{\boldsymbol{x}}\big(\boldsymbol{x}\boldsymbol{x}^T\big) \le P_c\end{aligned} \tag{17}$$

where $P_c$ is the sum power constraint. Here, we assume that all the nodes, including the anchors and the target nodes, can receive effective signals when the system is deployed. Thus, the minimum received energy constraint is ignored. It is clearly observed that $\mathbb{P}_1$ is complicated to expand and it is also a monotonically nonincreasing function of $\mathbf{J}(\boldsymbol{\theta})$. Then, we apply the following propositions to relax the objectives:

*Proposition 2:* The SPEB satisfies that $\mathcal{P}(\boldsymbol{\theta}) \ge 4N_T^2(1/[\mathrm{tr}\{\mathbf{J}(\boldsymbol{\theta})\}])$. The "=" holds if and only if $\tau_1 = \tau_2 = \ldots = \tau_{2N_T}$, where $\tau_1, \tau_2, \ldots, \tau_{2N_T}$ are the eigenvalues of $\mathbf{J}(\boldsymbol{\theta})$.

*Proof:* Refer to Appendix B for the detailed derivation. ■

Using Proposition 2, $\mathbb{P}_1$ can be relaxed to the maximum $\mathrm{tr}\{\mathbf{J}(\boldsymbol{\theta})\}$ problem

$$\begin{aligned}(\mathbb{P}_1^*):\ &\max_{\boldsymbol{x}}\ \mathrm{tr}\{\mathbf{J}(\boldsymbol{\theta})\}\\ &\text{s.t.}\ \ \mathbb{E}_{\boldsymbol{x}}(\boldsymbol{x}\boldsymbol{x}^T) \le P_c\end{aligned} \tag{18}$$

where $\mathrm{tr}\{\mathbf{J}(\boldsymbol{\theta})\}$ is derived according to (56) in Appendix B:

$$\mathrm{tr}\{\mathbf{J}(\boldsymbol{\theta})\} = \boldsymbol{x}^T\left(\mathbf{G}_A^T\sum_{i=1}^{N_T}\Lambda_i\mathbf{G}_A + \mathbf{G}_C^T\left(\sum_{i=1}^{N_T}\Gamma_i + \Xi\right)\mathbf{G}_C\right)\boldsymbol{x} \tag{19}$$

and $\Lambda_i$, $\Gamma_i$, and $\Xi$ are derived in (57), (58), and (60).

### B. Close-Form Solution

The above objective is a typical QCQP. One feasible solution is to use Lagrangian relaxation and Lagrangian multiplier method to approximate the optimal value. Here, we define $\Psi = \mathbf{G}_A^T\sum_{i=1}^{N_T}\Lambda_i\mathbf{G}_A + \mathbf{G}_C^T(\sum_{i=1}^{N_T}\Gamma_i + \Xi)\mathbf{G}_C$, and it is clear that $\Psi$ is a positive-defined matrix due to the nature of FIM. Then, we define the multiplier $\mu > 0$, and construct the Lagrangian function of $\mathbb{P}_1^*$ as follows:

$$\mathcal{F}_1(\boldsymbol{x}, \mu) = -\boldsymbol{x}^T\Psi\boldsymbol{x} - \mu\big(P_c - \boldsymbol{x}^T\boldsymbol{x}\big) \tag{20}$$

where we convert the objective $\max_{\boldsymbol{x}} \mathrm{tr}\{\mathbf{J}(\boldsymbol{\theta})\}$ into $\min_{\boldsymbol{x}} -\mathrm{tr}\{\mathbf{J}(\boldsymbol{\theta})\}$. Then, the Karush–Kuhn–Tucker (KKT) conditions are attained

$$\frac{\partial\mathcal{F}_1(\boldsymbol{x}, \mu)}{\partial\boldsymbol{x}} = -\Psi\boldsymbol{x} + \mu\boldsymbol{x}^T\boldsymbol{x} = 0. \tag{21}$$

Since $\mu \neq 0$, we have

$$\Psi\boldsymbol{x} = \mu\boldsymbol{x}. \tag{22}$$

According to the definition of the matrix eigenvalue, it is obvious that $\mu$ is one of the eigenvalues for matrix $\Psi$, and $\boldsymbol{x}$ is the corresponding eigenvector. Since $\Psi$ is a positive semidefinite Hermitian matrix, it can be eigendecomposed to $\Psi = \mathbf{Q}\Phi\mathbf{Q}^T$, where $\mathbf{Q}$ is the unitary matrix and $\Phi$ is a diagonal matrix of the eigenvalues of $\Psi$. Then, define $\acute{\boldsymbol{x}} = \mathbf{Q}^T\boldsymbol{x}$, and $\varsigma_1, \ldots, \varsigma_K$ are the real and nonnegative eigenvalues of $\Psi$. Then, we have $\boldsymbol{x}^T\Psi\boldsymbol{x} = \sum_k \varsigma_k|\acute{x}_k|^2$, where $\acute{\boldsymbol{x}} = (0, \ldots, 0, \acute{x}_k, 0, \ldots, 0)$, and $|\acute{x}_k|^2 = 1$. In this case, the maximal $\boldsymbol{x}^T\Psi\boldsymbol{x}$ is attained with $\varsigma_{max} = \arg\max\{\varsigma_1, \ldots, \varsigma_K\}$. Thus, the optimal solution $\boldsymbol{x}^{\mathrm{opt}}$ is proportional to the corresponding column of $\mathbf{Q}$. Considering the power constraint $P_c$, the optimal $\boldsymbol{x}^{\mathrm{opt}} = c \cdot \mathrm{maxeig}(\Psi)$, where $c$ is an adapting co-efficient to make the sum of signal power approach $P_c$.

### C. Energy Efficiency Optimization

The energy efficiency problem in the cooperative localization of WPCN is to achieve the minimum Tx power of E-AP with given localization requirements constraints. The localization requirements mean that the estimation error of each node should not exceed a typical threshold, which is defined as $\rho_{th}$. Thus, the energy efficiency problem is expressed as

$$\begin{aligned}(\mathbb{P}_2):\ &\min_{\boldsymbol{x}}\ \mathbb{E}_{\boldsymbol{x}}\big(\boldsymbol{x}\boldsymbol{x}^T\big)\\ &\text{s.t.}\ \ \mathcal{P}(\boldsymbol{\theta}) \le N_T\rho_{th}\end{aligned} \tag{23}$$

where the localization should satisfy the average localization requirements. Similar to $\mathbb{P}_1$, we can relax $\mathbb{P}_2$ according to Proposition 2

$$\begin{aligned}\big(\mathbb{P}_2^*\big):\ &\min_{\boldsymbol{x}}\ \mathbb{E}_{\boldsymbol{x}}\big(\boldsymbol{x}\boldsymbol{x}^T\big)\\ &\text{s.t.}\ \ \boldsymbol{x}^T\left(\mathbf{G}_A^T\sum_{i=1}^{N_T}\Lambda_i\mathbf{G}_A + \mathbf{G}_C^T\left(\sum_{i=1}^{N_T}\Gamma_i + \Xi\right)\mathbf{G}_C\right)\boldsymbol{x}\\ &\qquad \ge \frac{4N_T}{\rho_{th}}.\end{aligned} \tag{24}$$

However, $\mathbb{P}_2^*$ cannot provide a closed-form solution, since it may not be always convex. Thus, we employ the SDP to relax such a problem. First, let $\mathbf{X} = \boldsymbol{x}^T\boldsymbol{x}$ and it is obvious that $\mathrm{rank}(\mathbf{X}) = 1$. Consider $\boldsymbol{x}\boldsymbol{x}^T = \mathrm{tr}(\mathbf{X})$ and $\boldsymbol{x}^T\Omega\boldsymbol{x} = \mathrm{tr}(\mathbf{Q}\mathbf{X})$, where $\Omega$ indicates any symmetric matrix, then $\mathbb{P}_2^*$ is equivalent to

$$\begin{aligned}(\widetilde{\mathbb{P}}_2^*):\ &\min_{\mathbf{X}}\ \mathrm{tr}(\mathbf{X})\\ &\text{s.t.}\ \ \mathrm{tr}\left(\left(\mathbf{G}_A^T\sum_{i=1}^{N_T}\Lambda_i\mathbf{G}_A + \mathbf{G}_C^T\left(\sum_{i=1}^{N_T}\Gamma_i + \Xi\right)\mathbf{G}_C\right)\mathbf{X}\right)\end{aligned}$$

$$\geq \frac{4N_T}{\rho_{th}}$$
$$\mathbf{X} \geq \mathbf{0} \tag{25}$$

which is a typical SDP problem and can be solved by many efficient tools, e.g., CVX. When $\mathbf{X}$ is attained, we have $\mathbf{X} = \lambda_0 \mathbf{q}_0 \mathbf{q}_0^T$, where $\lambda_0$ is the eigenvalue of rank one matrix and $\mathbf{q}_0$ is the corresponding eigenvector. Then, the feasible solution of $\boldsymbol{x}$ is $\boldsymbol{x}^* = \sqrt{\lambda_0}\mathbf{q}_0$.

### D. Calibrations

Note that using Proposition 2 to solve $(\widetilde{\mathbb{P}}_2^*)$ can only meet a loose bound of the localization requirement, since several relaxations are employed. Thus, the localization requirement constraints are not met even if the optimal solutions are attained. However, such loose bound can be adapted into a tight bound by introducing a coefficient $c_0$ to $(4N_T/\rho_{th})$, which means that we can set a value during the computation to force the relaxed constraints strictly approach the real localization requirements. Therefore, we employ a self-calibration method and divide the SDP solutions into two steps. In the first step, we set $c_0 = 1$, and turn $(\widetilde{\mathbb{P}}_2^*)$ as follows:

$$\begin{aligned}(\widetilde{\mathbb{P}}_{2-c}^*): \ &\min_{\mathbf{X}} \ \mathrm{tr}(\mathbf{X}) \\ &\text{s.t.} \ \mathrm{tr}\left(\left(\mathbf{G}_A^T \sum_{i=1}^{N_T} \Lambda_i \mathbf{G}_A + \mathbf{G}_C^T \left(\sum_{i=1}^{N_T} \Gamma_i + \Xi\right)\mathbf{G}_C\right)\mathbf{X}\right) \\ &\quad \geq \frac{c_0}{\rho_{th} N_T} \\ &\quad \mathbf{X} \geq \mathbf{0}\end{aligned} \tag{26}$$

where we change $(4N_T/\rho_{th})$ into $(c_0/[\rho_{th}N_T])$ in order to simplify the further calibration and approach the real localization requirements. When the optimal solution $\boldsymbol{x}^*$ is attained, we substitute $\boldsymbol{x}^*$ into (11). Then, we attain a real trace of FIM $\widetilde{\rho} = \mathbf{J}^{-1}(\boldsymbol{\theta}|\boldsymbol{x}^*)$ based on $\boldsymbol{x}^*$, and we set $c_0 = [\widetilde{\rho}/(\rho_{th}N_T)]$. The final optimal solution is attained when the SDP of $\widetilde{\mathbb{P}}_{2-c}^*$ is executed again with new $c_0$, and the localization requirements are met as well.

## V. Spatial Recursive Formulations for Single Target

### A. Spatial Recursive Optimization

When the $N_T + 1$th node joins the network, the other nodes will send the ranging signals to help this node attain its initial location. However, the ranging signals for the other $N_T$ node localizations are not exploited. Then, we define the whole estimated vector as $\boldsymbol{\theta}_s = [\mathbf{p}_{N_T+1}^T \ \mathbf{p}_1^T \ \mathbf{p}_2^T \ \cdots \ \mathbf{p}_{N_T}^T]^T = [\mathbf{p}_{N_T+1}^T \ \boldsymbol{\theta}^T]^T$. The FIM is formulated as (28), shown at the bottom of the page, and using the Shur complement, we have (29), shown at the bottom of the page, where

$$\begin{cases} \mathbf{C}_{N_T+1,i} = \mathbf{C}_{i,N_T+1} = \left(\lambda_{N_T+1,i} + \lambda_{i,N_T+1}\right)\mathbf{J}\left(\phi_{N_T+1,i}\right) \\ \mathbf{M}_{N_T+1} = \left[-\mathbf{C}_{N_T+1,1} \ -\mathbf{C}_{N_T+1,2} \ \cdots \ -\mathbf{C}_{N_T+1,N_T}\right] \end{cases} \tag{27}$$

and $\mathbf{I}_{N_T \times N_T}$ is the identical matrix with $N_T \times N_T$ dimensions, and $\otimes$ is the Kronecker product.

However, using such FIM of optimization will lead to higher order programming, which is too complicated to solve. Thus, we derive a new upper bound of $\mathbf{J}(\mathbf{p}_{N_T+1})$ by ignoring some parts of $\mathbf{J}(\mathbf{p}_{N_T+1})$, which is

$$\mathbf{J}_U(\mathbf{p}_{N_T+1}) = \mathbf{J}_A(\mathbf{p}_{N_T+1}) + \sum_{i \neq N_T+1} \mathbf{C}_{N_T+1,i} \tag{30}$$

Using the elementary algebra, we obtain the inequality

$$\mathbf{J}(\boldsymbol{\theta}_s) \preceq \mathbf{J}_U(\boldsymbol{\theta}_s) \tag{31}$$

Then, we attain the lower bound $\mathcal{P}(\mathbf{p}_{N_T+1}) \geq \mathcal{P}_L(\mathbf{p}_{N_T+1}) = \mathrm{tr}\left(\mathbf{J}_U^{-1}(\mathbf{p}_{N_T+1})\right)$. Thus, we can use the minimum $\mathcal{P}_L(\mathbf{p}_{N_T+1})$ to indicate the lower bound of $\mathcal{P}(\mathbf{p}_{N_T+1})$. In this case, we just need to attain the maximum $\mathrm{tr}\left(\mathbf{J}_U(\mathbf{p}_{N_T+1})\right)$.

Using Proposition 2, the spatial recursive beamforming is formulated as

$$\begin{aligned}(\mathbb{P}_3^*): \ &\max_{\boldsymbol{x}} \ \mathrm{tr}\{\mathbf{J}_U(\mathbf{p}_{N_T+1})\} \\ &\text{s.t.} \ \mathbb{E}_{\boldsymbol{x}}(\boldsymbol{x}\boldsymbol{x}^T) \leq P_c\end{aligned} \tag{32}$$

which is also QCQP. Similar to $\mathbb{P}_1^*$, $\mathrm{tr}\{\mathbf{J}_U(\mathbf{p}_{N_T+1})\}$ is a simplified form according to (19)

$$\mathrm{tr}\left\{\mathbf{J}_U\left(\mathbf{p}_{N_T+1}\right)\right\} = \boldsymbol{x}^T\left(\mathbf{G}_A^T \Lambda_{N_T+1}\mathbf{G}_A + \mathbf{G}_C^T\left(\sum_{i=1}^{N_T}\Gamma_i\right)\mathbf{G}_C\right)\boldsymbol{x}. \tag{33}$$

Similarly, we can construct KKT conditions just like (21), and use eigenvalue decomposition to attain the optimal vector $\boldsymbol{x}^*$.

### B. Energy Efficiency Problem

For energy efficiency purpose, we still use $\mathbf{J}_U(\mathbf{p}_{N_T+1})$ to relax $\mathbf{J}(\mathbf{p}_{N_T+1})$. Although such relaxation is not tight, the computation overhead is efficiently reduced. Then, using Proposition 2, the objective is expressed as

$$\begin{aligned}(\mathbb{P}_4^*): \ &\min_{\boldsymbol{x}} \ \mathbb{E}_{\boldsymbol{x}}(\boldsymbol{x}\boldsymbol{x}^T) \\ &\text{s.t.} \ \mathrm{tr}\left\{\mathbf{J}_U(\mathbf{p}_{N_T+1})\right\} \geq \frac{4}{\rho_{th}}.\end{aligned} \tag{34}$$

$$\mathbf{J}(\boldsymbol{\theta}_s) = \begin{pmatrix} \mathbf{J}_A(\mathbf{p}_{N_T+1}) + \sum_{i \neq N_T+1} \mathbf{C}_{N_T+1,i} & -\mathbf{C}_{N_T+1,1} & \cdots & -\mathbf{C}_{N_T+1,N_T} \\ -\mathbf{C}_{1,N_T+1} & \mathbf{J}_A(\mathbf{p}_1) + \sum_{i \neq 1} \mathbf{C}_{1,i} & \cdots & -\mathbf{C}_{1,N_T} \\ \vdots & \vdots & \ddots & \vdots \\ -\mathbf{C}_{N_T,N_T+1} & -\mathbf{C}_{N_T,1} & \cdots & \mathbf{J}_A(\mathbf{p}_{N_T}) + \sum_{i \neq N_T} \mathbf{C}_{N_T,i} \end{pmatrix} \tag{28}$$

$$\mathbf{J}(\mathbf{p}_{N_T+1}) = \mathbf{J}_A(\mathbf{p}_{N_T+1}) + \sum_{i \neq N_T+1} \mathbf{C}_{N_T+1,i} - \mathbf{M}_{N_T+1}(\mathbf{J}(\boldsymbol{\theta}) + \mathbf{I}_{N_T \times N_T} \otimes \mathbf{M}_{N_T+1})^{-1}\mathbf{M}_{N_T+1}^T \tag{29}$$

Similar to $\mathbb{P}_2^*$, we employ $\mathbf{X} = \boldsymbol{x}^T\boldsymbol{x}$ to relax $\mathbb{P}_4^*$ and we attain the SDP formulations:

$$(\widetilde{\mathbb{P}}_4^*): \min_{\mathbf{X}} \ \mathrm{tr}(\mathbf{X}) \quad \text{s.t.} \ \mathrm{tr}\{\mathbf{J}_U(\mathbf{p}_{N_T+1})\} \geq \frac{4}{\rho_{th}} \quad \mathbf{X} \geq \mathbf{0} \tag{35}$$

which can also be solved by CVX.

### C. Calibration

Note that $\widetilde{\mathbb{P}}_4^*$ still attains a loose bound of the localization requirements. In this case, a two-step calibration method which is similar to $\mathbb{P}_2^*$ is developed. In this calibration, we also employ a coefficient $c_0$ to adapt the constraints. The first step is to set $c_0 = 1$ and we obtain

$$(\widetilde{\mathbb{P}}_{4-c}^*): \min_{\mathbf{X}} \ \mathrm{tr}(\mathbf{X}) \quad \text{s.t.} \ \mathrm{tr}\{\mathbf{J}_U(\mathbf{p}_{N_T+1})\} \geq \frac{c_0}{\rho_{th}} \quad \mathbf{X} \geq \mathbf{0}. \tag{36}$$

Then, the initial optimal solution $\boldsymbol{x}^*$ is attained. In the second step, we use $\boldsymbol{x}^*$ to derive the actual trace of $\mathbf{J}(\mathbf{p}_{N_T+1})$, and compute $\widetilde{\rho} = \mathbf{J}^{-1}(\mathbf{p}_{N_T+1})$. Then, we still set $c_0 = (\widetilde{\rho}/\rho_{th})$ and use SDP to attain the final solution of $\widetilde{\mathbb{P}}_{4-c}^*$.

## VI. Channel Uncertainty

In the real applications, the channel states are time-varying and interfered by the noise. Thus, the beamforming schemes should also consider the channel uncertainty problem. Then, the optimizations are reformulated accordingly and the impact of the uncertainty should be analyzed.

Considering that the $k$th antenna sends the pilot signal with power $q_k$ to node $n$, node $n$ will estimate the channel state and feedback to the E-AP. The minimum MSE (MMSE) of $g_{kn}$ is denoted by $\tilde{g}_{kn}$, and the estimation error is $e_{kn} \triangleq \tilde{g}_{kn} - g_{kn}$, which is a random variables with zero mean and variance [46]

$$\sigma_{kn}^2 = \frac{\beta_{kn}}{1 + \beta_{kn} L q_k/\sigma^2} \tag{37}$$

where $\beta_{kn}$ is the path loss from antenna $k$ to node $n$, $L$ indicates the symbol length and $\sigma^2$ is the background noise variance. Considering the estimation error is independent and identically distributed (i.i.d.), it is easily attained $||g_{kn}||^2 = ||\tilde{g}_{kn}||^2 + \sigma_{kn}^2$, and $\mathbb{E}(g_{kn}g_{km}) = \tilde{g}_{kn}\tilde{g}_{km}$. Then, we update the received power for node $n$ in (2) with the channel uncertainty model

$$\tilde{r}_y^n = \boldsymbol{x}^T \begin{pmatrix} ||\tilde{g}_{1n}||^2 + \sigma_{1n}^2 & \tilde{g}_{1n}\tilde{g}_{2n} & \cdots & \tilde{g}_{1n}\tilde{g}_{Kn} \\ \tilde{g}_{2n}\tilde{g}_{1n} & ||\tilde{g}_{2n}||^2 + \sigma_{2n}^2 & \cdots & \tilde{g}_{2n}\tilde{g}_{Kn} \\ \vdots & \vdots & \ddots & \vdots \\ \tilde{g}_{Kn}\tilde{g}_{1n} & \tilde{g}_{Kn}\tilde{g}_{2n} & \cdots & ||\tilde{g}_{Kn}||^2 + \sigma_{Kn}^2 \end{pmatrix} \boldsymbol{x} \tag{38}$$

Statistically, $\tilde{g}_{kn}\tilde{g}_{km}$ is equivalent to $g_{kn}g_{km}$. In this case, the FIM and the localization estimation accuracy does not only rely on the channel state but also depends on the estimation error of the wireless power propagation channel. The estimation error mainly influences the diagonal elements in $\tilde{r}_y^n$. To simplify the analysis, we mainly use the pilot signal-to-noise-ratio (SNR) as the main parameter to indicate the channel uncertainty.

## VII. Simulation

The proposed schemes are evaluated by extensive simulations. In the simulations, we assume that all nodes, including ten anchors and several targets are randomly deployed in a $500 \times 500$ m$^2$ playing field. The antenna array of E-AP can be deployed in the center of the playing field or randomly deployed throughout the whole playing field. The signal carrier frequency is 2.4 GHz and the maximum allowed transmitted power of E-AP is 30 dBm (1 W). In addition, the received power of each node for communications and harvesting energy is -90 dBm, and the power of the background noise is -130 dBm. We assume a free-space propagation model of the wireless power transfer channel, and the NLOS ranging is not considered in FIM calculation [3].

We use SPEB to indicate the localization accuracy and use the total transmitted power of E-AP as the energy efficiency metric. Since our schemes are to relax the trace of FIM and employ quadratic programming or SDP to solve the optimization problems, our schemes are indicated as Tr-QP or Tr-SDP. The proposed schemes are compared with equally combining scheme (EC), which allocates the transmitted power equally and the same wave form on each antenna, and SDP-based power allocation schemes in [14], [39], and [40].

To transfer the power allocation from WCN to WPCN, we consider the signals from E-AP is orthogonal $\mathbb{E}(\sum_{k\neq l} x_k x_l) = 0$. Then, $r_y^n = \mathbb{E}(\sum_{k=1}^K ||g_{kn}||^2 ||x_k||^2)$. Define the channel power gain vector for the node $n$ $\bar{\mathbf{g}}_n = [\mathbb{E}(||g_{1n}||^2),\ \mathbb{E}(||g_{1n}||^2), \ldots,\ \mathbb{E}(||g_{Kn}||^2)]^T$, and define $\mathbf{r}_x = [r_x^1,\ r_x^2, \ldots,\ r_x^K]$ as the transmitter power vector of $\boldsymbol{x}$, where $r_x^k = \mathbb{E}(||x_k||^2),\ k \in \{1,\ 2,\ \ldots,\ K\}$. Then, we have

$$r_y^n = \bar{\mathbf{g}}_n^T \mathbf{r}_x \tag{39}$$

It is clearly observed that $r_y^n$ is determined by the power allocation of $\mathbf{r}_x$. Then, we reformulate $\mathbf{J}(\boldsymbol{\theta}|\mathbf{r}_x)$ and substitute it into $\mathbf{J}(\boldsymbol{\theta})$ in the problem formulations. We also employ $\mathbf{r}_x$ to indicate $\mathbb{E}_{\boldsymbol{x}}(\boldsymbol{x}\boldsymbol{x}^T)$. In this case, the energy beamforming problem is converted into a power allocation problem. For SDP solutions, one optional method is to employ an auxiliary covariance matrix $\mathbf{Z}$ [39], which satisfies that $\mathbf{J}^{-1}(\boldsymbol{\theta}|\mathbf{r}_x) \succeq \mathbf{Z}^{-1}$. Using the linear matrix inequality (LMI), we have

$$\begin{pmatrix} \mathbf{J}(\boldsymbol{\theta}|\mathbf{r}_x) & \mathbf{I} \\ \mathbf{I} & \mathbf{Z} \end{pmatrix} \succeq \mathbf{0} \tag{40}$$

where $\mathbf{I}$ is the identical matrix with the same dimension of $\mathbf{J}(\boldsymbol{\theta}|\mathbf{r}_x)$ and $\mathbf{Z}$. Then, we can use $\mathbf{Z}$ either as the objective or localization requirement, which is a typical SDP problem. However, such a method is over relaxed and far from the actual FIM value, especially in the cooperative localization framework. Thus, we still employ the trace of $\mathbf{J}(\boldsymbol{\theta}|\mathbf{r}_x)$ and reformulate the objectives, which are still SDP problems.

### A. Full Connected Network Evaluation

First, the beamforming strategies for cooperative localization of WPCN are evaluated in a sequential way, in which

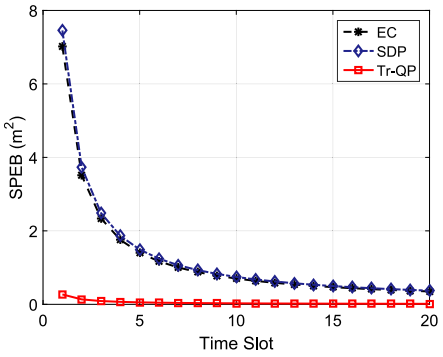


Fig. 2. Sequential evaluation of SPEB. The SPEB contains the previous FIM.

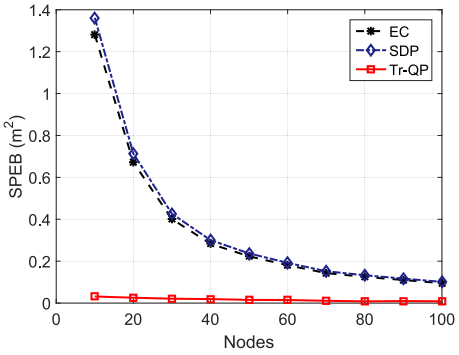


Fig. 3. Cooperative node evaluation. We increase the nodes to check whether it will benefit the localization performance.

the nodes harvest the energy from beamformed microwaves and exchange signals during each time slots, and then fuse the previous FIM to derive the current SPEBs. The averaged SPEBs of all the schemes are illustrated in Fig. 2. It is clearly observed that the estimation error of Tr-QP is much lower than the other two. Compare with SDP, Tr-QP can effectively use the spatial correlations to increase the performance. While the results of SDP only allocate the major power on one antenna, which ignores the benefits of the correlated channels. In this case, SDP is even slightly worse than EC. However, with the previous information, the SPEBs of three schemes gradually converge to a quite low value.

Then, we increase the cooperative nodes from 10 to 100. As illustrated in Fig. 3, the SPEBs of all three schemes drop down with more nodes participating in the localization. The Tr-QP outperforms other schemes even with only 10 cooperative nodes, and the related SPEB only decreases a limited value with more cooperative nodes.

Next, we adapt the antennas of E-AP to examine the impacts for cooperative localizations. In this simulation, we also evaluate the impacts of both centralized and distributed antennas of E-APs. For centralized antennas, we assume there is only one E-AP with a Tx antenna array that is deployed in the center of the playing field. For distributed antennas, we assume multiple E-APs randomly deployed in the whole playing field and each E-AP contains only one antenna. We adapt the number of antennas from 4 to 64. The SPEBs of three schemes in both cases are depicted in Fig. 4. For EC and SDP schemes, the distributed antennas outperform the centralized antennas. In addition, more antennas can benefit both schemes. However,

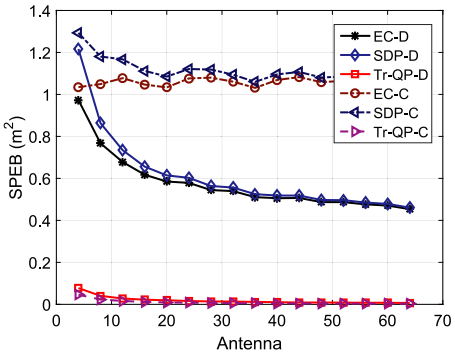


Fig. 4. SPEBs with different antennas of E-APs. In this simulation, we consider both centralized and distributed antennas.

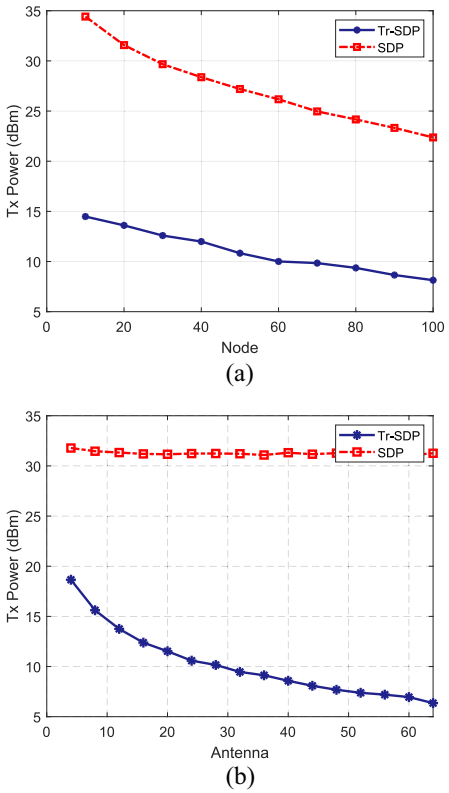


Fig. 5. Energy efficiency evaluation for full connected network. (a) Tx power consumption with different number of cooperative nodes. (b) Tx power consumption with different number of antennas.

the SPEBs of Tr-QP in both cases are quite similar, and the centralized antenna array is slightly better than the distributed antennas. Increasing the number of antennas reduces the SPEBs of Tr-QP but not too much since the initial values are below 0.1 with only four antennas.

Furthermore, we evaluate the power consumptions of our proposed energy efficiency schemes. We compare our SDP-based scheme, which is named by Tr-SDP, with the SDP-based power allocation scheme. The average SPEB requirement is 1 m$^2$. The cooperative node number and the antenna number are also adapted to evaluate the performance, in which the SPEB is used to indicate localization accuracy and the total Tx power (dBm) is the energy efficiency metric. The results are depicted in Fig. 5. As illustrated in Fig. 5(a) and (b), the

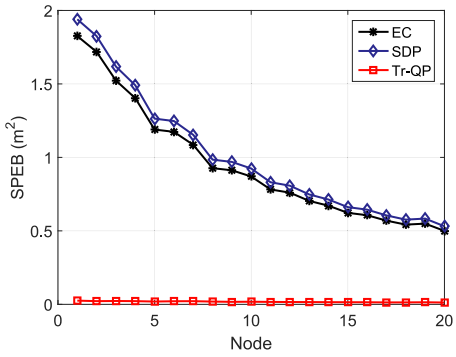


Fig. 6. SPEBs for single-node evaluation.

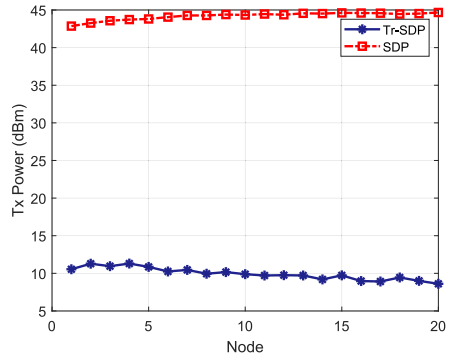


Fig. 7. Tx power consumptions for single-node evaluation.

total Tx power of Tr-SDP is lower than SDP. With the participation of more nodes and antennas, the power consumptions are gradually reduced.

### B. Spatial Recursive Evaluation

In the spatial recursive simulation, the nodes join the network one by one, and we apply the proposed scheme to attain the optimal SPEB of the new node. The number of anchors is 10. The power constraint is 30 dBm for optimal localization problems, and we employ the spatial recursive form of Tr-QP to solve $\mathbb{P}_3^*$. We also compare our scheme with SDP and EC for a single node. As indicated in Fig. 6, the SPEBs of SDP and EC are decreasing when more nodes join the network. However, the Tr-QP maintains a low value which is below 0.2 when the network only contains one node, and such value is kept even with more nodes joining the network, which outperforms the other two schemes.

For energy efficiency optimization, the localization requirement constraint is 1 m$^2$, and we apply Tr-SDP to solve $\widetilde{\mathbb{P}}_4^*$. We also compare our scheme with SDP schemes, and the power consumptions are illustrated in Fig. 7, in which Tr-SDP consumes less power than SDP and such a value even drops with more nodes.

### C. Channel Uncertainty Evaluation

Finally, we introduce the channel uncertainty model into the simulations to evaluate the impacts. We still use ten anchors and 20 nodes, and the simulation parameters are the same as mentioned before. For channel estimations, the accuracy

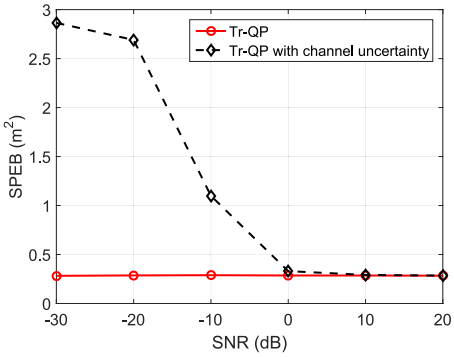


Fig. 8. SPEB evaluation with channel uncertainty.

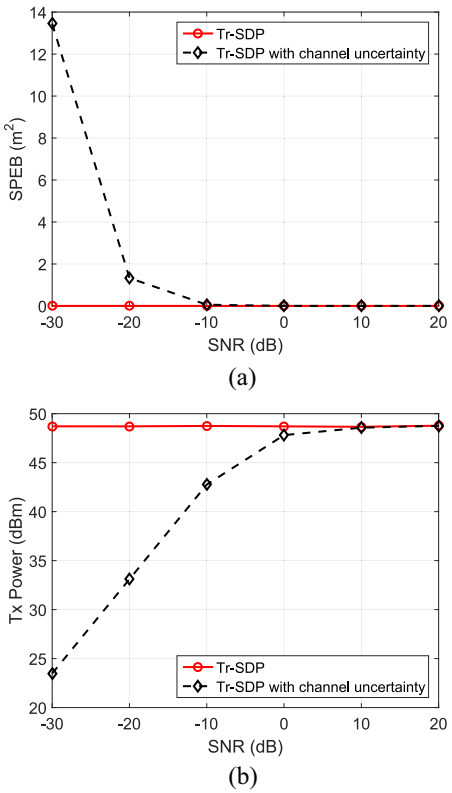


Fig. 9. Energy efficiency evaluation with channel uncertainty. (a) SPEB results. (b) Tx power consumption.

mainly relies on the transmitted pilot power and the noise. Therefore, we employ the pilot SNR to indicate the channel estimation parameter. Then, we adapt the SNR from -30 to 20 dB, and both Tr-QP for the optimal localization and Tr-SDP for energy efficiency are analyzed. In Fig. 8, the SPEB of Tr-QP with lower SNR is higher than the Tr-QP with ideal channel information, which demonstrates the degrading localization accuracy due to the inaccurate channel estimation. When the SNR is increased, the SEPB with channel uncertainty is gradually reduced and approaching the ideal case.

Such impacts also lead to unreliable energy consumptions, as illustrated in Fig. 9(a). The SPEB of Tr-SDP with lower SNR is much higher than the ideal channel case, which indicates that the localization requirements are not guaranteed and SPEBs are wrongly derived. The Tx power is reduced

with higher SPEBs. However, such power reduction is mainly caused by the unreliable SPEB due to the channel uncertainty, because the localization requirement constraints are not bounded any more during the SDP calculations. In this case, the system consumes less power compared with an ideal case, because it considers the required localization accuracy is already achieved.

## VIII. Conclusion

In this article, we analyzed the fundamental limits of the cooperative localization in WPCNs. We formulated the cooperative FIM and proposed the beamforming schemes to solve the localization accuracy and energy efficiency optimization problems. In addition, the spatial recursive form and related beamforming schemes were also investigated. The simulations demonstrated that our schemes outperform the power allocation-based SDP methods and equally combining power scheme. With more nodes and more antennas of E-AP participating, the localization accuracy is increased. We also observe that the channel uncertainty affect the localization accuracy and consume more power to achieve the localization requirements.

## Appendix A
## FIM for Cooperative Localization in WPCN

According to (8), the log likelihood function for $\theta$ consists of two parts

$$\ln f(z|\boldsymbol{\theta}) = \ln f(z_A|\boldsymbol{\theta}) + \ln f(z_C|\boldsymbol{\theta}). \tag{41}$$

For the first part $\ln f(z_A|\boldsymbol{\theta})$, the score function is (42), shown at the top of the next page, where $\ln f(z_i^A|\boldsymbol{p}_i) = \sum_{j=1}^{N_A} \ln f(z_{j,i}|\boldsymbol{p}_i)$ is the sum log likelihood for $\boldsymbol{p}_i$ based on the observations from anchors.

Due to the independence of the received signals for different target nodes, $([\partial \ln f(z_m^A|\boldsymbol{p}_i)]/\partial \boldsymbol{p}_i) = 0, m \neq i$, then we have a diagonal matrix

$$\mathbf{U}_A(\boldsymbol{\theta}) = \begin{pmatrix} \frac{\partial \ln f(z_1^A|\boldsymbol{p}_1)}{\partial \boldsymbol{p}_1} & & \\ & \ddots & \\ & & \frac{\partial \ln f(z_{N_T}^A|\boldsymbol{p}_{N_T})}{\partial \boldsymbol{p}_{N_T}}. \end{pmatrix} \tag{43}$$

For each $([\partial \ln f(z_{j,i}|\boldsymbol{p}_i)]/\partial \boldsymbol{p}_i)$, we decompose it according to the chain rule

$$\frac{\partial \ln f(z_{j,i}|\boldsymbol{p}_i)}{\partial \boldsymbol{p}_i} = y_j \cdot \frac{\partial h_{j,i}(d_{j,i})}{\partial d_{j,i}} \cdot \mathbf{q}_{j,i} \tag{44}$$

where $\mathbf{q}_{j,i} = [\cos\phi_{j,i} \quad \sin\phi_{j,i}]^T$ with $\phi_{j,i} = \arctan[(p_i^X - p_j^X)/(p_i^Y - p_j^Y)]$. Here, we consider a flat fading channel, in which the path loss follows:

$$r_z^{j,i} = r_y^j \left(\frac{f_c}{4\pi d_{j,i}}\right)^{2\beta} \xi_{j,i} \tag{45}$$

where $r_z^{j,i}$ indicates the received signal power from anchor $j$ to target $i$, and $f_c$ represents the central frequency of the signal. If the signal noise follows the zero-mean Gaussian distribution with power $N_0$, we have:

$$\mathbb{E}\left(\frac{\partial \ln f(z_{j,i}|\boldsymbol{p}_i)}{\partial \boldsymbol{p}_i} \frac{\partial \ln f(z_{j,i}|\boldsymbol{p}_i)}{\partial \boldsymbol{p}_i}^T\right) = r_y^j \frac{\xi_{j,i}\beta^2(\frac{f_c}{4\pi})^{2\beta}}{d_{j,i}^{2\beta+2}N_0}\mathbf{J}(\phi_{j,i}) \tag{46}$$

where $\mathbf{J}(\phi_{j,i}) = \mathbf{q}_{j,i}\mathbf{q}_{j,i}^T$ and $r_y^j$ is attained according to (2). Then, we employ $\lambda_{j,i}$ to indicate the ERC

$$\lambda_{j,i} = \mathbb{E}_{\boldsymbol{x}}\left(\boldsymbol{x}^T\mathbf{g}_j^T\mathbf{g}_j\boldsymbol{x}\right)\frac{\xi_{j,i}\beta^2\left(\frac{f_c}{4\pi}\right)^{2\beta}}{d_{j,i}^{2\beta+2}N_0} \tag{47}$$

and we obtain $\mathbf{J}_A(\boldsymbol{p}_i)$

$$\mathbf{J}_A(\boldsymbol{p}_i) = \mathbb{E}(\frac{\partial \ln f(z_i^A|\boldsymbol{p}_i)}{\partial \boldsymbol{p}_i} \frac{\partial \ln f(z_i^A|\boldsymbol{p}_i)}{\partial \boldsymbol{p}_i}^T) = \sum_{j=1}^{N_T} \lambda_{j,i}\mathbf{J}(\phi_{j,i}). \tag{48}$$

Then, $\mathbf{J}_A(\boldsymbol{\theta}) = \mathbf{diag}(\mathbf{J}_A(\boldsymbol{p}_1), \ldots, \mathbf{J}_A(\boldsymbol{p}_{N_T}))$ is attained.

Similarly, we have $\mathbf{U}_C(\boldsymbol{\theta}) = \nabla_{\boldsymbol{\theta}} \ln f(\boldsymbol{z}_C|\boldsymbol{\theta})$ and attain (49), shown at the top of the next page, where $\ln f(z_i^C|\boldsymbol{p}_i) = \sum_{m=1}^{N_T} \ln f(z_{m,i}|\boldsymbol{p}_i)$ is the sum log likelihood for $\boldsymbol{p}_i$ based on the observations sending from all the target nodes to target $i$. In addition, $([\partial \ln f(z_m^C|\boldsymbol{p}_i)]/\partial \boldsymbol{p}_i) = ([\partial \ln f(z_{i,m}|\boldsymbol{p}_i)]/\partial \boldsymbol{p}_i), m \neq i$. Then, $\mathbf{U}_C(\boldsymbol{\theta})$ is simplified as right-hand side form in (49).

For $([\partial \ln f(z_i^C|\boldsymbol{p}_i)]/\partial \boldsymbol{p}_i)$, we have similar results to $\ln f(z_i^A|\boldsymbol{p}_i)$, in which each $([\partial \ln f(z_{m,i}|\boldsymbol{p}_i)]/\partial \boldsymbol{p}_i), m \neq i$

$$\frac{\partial \ln f(z_{m,i}|\boldsymbol{p}_i)}{\partial \boldsymbol{p}_i} = y_m \cdot \frac{\partial h_{m,i}(d_{m,i})}{\partial d_{m,i}} \cdot \mathbf{q}_{m,i}. \tag{50}$$

Similarly, $([\partial \ln f(z_{i,m}|\boldsymbol{p}_i)]/\partial \boldsymbol{p}_i)$ is

$$\frac{\partial \ln f(z_{i,m}|\boldsymbol{p}_i)}{\partial \boldsymbol{p}_i} = y_i \cdot \frac{\partial h_{i,m}(d_{i,m})}{\partial d_{i,m}} \cdot \mathbf{q}_{i,m} \tag{51}$$

where $\mathbf{q}_{i,m} = -\mathbf{q}_{m,i}$. Then, substitute $([\partial \ln f(z_{i,m}|\boldsymbol{p}_i)]/\partial \boldsymbol{p}_i)$ and $([\partial \ln f(z_i^C|\boldsymbol{p}_i)]/\partial \boldsymbol{p}_i)$ into $\mathbf{J}_C(\boldsymbol{\theta}) = \mathbb{E}(\mathbf{U}_C(\boldsymbol{\theta})\mathbf{U}_C^T(\boldsymbol{\theta}))$, we have

$$\mathbf{J}_C(\boldsymbol{\theta}) = \begin{pmatrix} \sum_{m\neq 1}\mathbf{C}_{1,m} & -\mathbf{C}_{1,2} & \cdots & -\mathbf{C}_{1,N_T} \\ -\mathbf{C}_{1,2} & \sum_{m\neq 2}\mathbf{C}_{2,m} & \cdots & -\mathbf{C}_{2,N_T} \\ \vdots & \vdots & \ddots & \vdots \\ -\mathbf{C}_{1,N_T} & -\mathbf{C}_{2,N_T} & \cdots & \sum_{m\neq N_T}\mathbf{C}_{N_T,m} \end{pmatrix} \tag{52}$$

where $\mathbf{C}_{m,i} = (\lambda_{i,m} + \lambda_{m,i})\mathbf{J}(\phi_{m,i})$; $i \neq m \in \mathcal{N}_T$, and $\lambda_{i,m}$ is

$$\lambda_{m,i} = \mathbb{E}_{\boldsymbol{x}}(\boldsymbol{x}^T\mathbf{g}_m^T\mathbf{g}_m\boldsymbol{x})\frac{\xi_{m,i}\beta^2(\frac{f_c}{4\pi})^{2\beta}}{d_{m,i}^{2\beta+2}N_0}. \tag{53}$$

Then, $\mathbf{J}(\boldsymbol{\theta}) = \mathbf{J}_A(\boldsymbol{\theta}) + \mathbf{J}_C(\boldsymbol{\theta})$.

## Appendix B
## Proof and Derivation of Traces of $\mathbf{J}(\boldsymbol{\theta})$ and $\mathbf{J}^{-1}(\boldsymbol{\theta})$

We decompose $\mathbf{J}(\boldsymbol{\theta})$ as follows:

$$\mathbf{J}(\boldsymbol{\theta}) = \mathbf{U}_\psi \begin{pmatrix} \tau_1 & & & \\ & \tau_2 & & \\ & & \ddots & \\ & & & \tau_{2N_T} \end{pmatrix} \mathbf{U}_\psi^T \tag{54}$$

$$\mathbf{U}_A(\boldsymbol{\theta}) = \nabla_{\boldsymbol{\theta}} \ln f(z_A|\boldsymbol{\theta}) = \begin{pmatrix} \frac{\partial \ln f(z_1^A|\boldsymbol{p}_1)}{\partial \boldsymbol{p}_1} & \frac{\partial \ln f(z_2^A|\boldsymbol{p}_1)}{\partial \boldsymbol{p}_1} & \cdots & \frac{\partial \ln f(z_{N_T}^A|\boldsymbol{p}_1)}{\partial \boldsymbol{p}_1} \\ \frac{\partial \ln f(z_1^A|\boldsymbol{p}_2)}{\partial \boldsymbol{p}_2} & \frac{\partial \ln f(z_2^A|\boldsymbol{p}_2)}{\partial \boldsymbol{p}_2} & \cdots & \frac{\partial \ln f(z_{N_T}^A|\boldsymbol{p}_2)}{\partial \boldsymbol{p}_2} \\ \vdots & \vdots & \ddots & \vdots \\ \frac{\partial \ln f(z_1^A|\boldsymbol{p}_{N_T})}{\partial \boldsymbol{p}_{N_T}} & \frac{\partial \ln f(z_2^A|\boldsymbol{p}_{N_T})}{\partial \boldsymbol{p}_{N_T}} & \cdots & \frac{\partial \ln f(z_{N_T}^A|\boldsymbol{p}_{N_T})}{\partial \boldsymbol{p}_{N_T}}. \end{pmatrix} \tag{42}$$

$$\mathbf{U}_C(\boldsymbol{\theta}) = \begin{pmatrix} \frac{\partial \ln f(z_1^C|\boldsymbol{p}_1)}{\partial \boldsymbol{p}_1} & \frac{\partial \ln f(z_2^C|\boldsymbol{p}_1)}{\partial \boldsymbol{p}_1} & \cdots & \frac{\partial \ln f(z_{N_T}^C|\boldsymbol{p}_1)}{\partial \boldsymbol{p}_1} \\ \frac{\partial \ln f(z_1^C|\boldsymbol{p}_2)}{\partial \boldsymbol{p}_2} & \frac{\partial \ln f(z_2^C|\boldsymbol{p}_2)}{\partial \boldsymbol{p}_2} & \cdots & \frac{\partial \ln f(z_{N_T}^C|\boldsymbol{p}_2)}{\partial \boldsymbol{p}_2} \\ \vdots & \vdots & \ddots & \vdots \\ \frac{\partial \ln f(z_1^C|\boldsymbol{p}_{N_T})}{\partial \boldsymbol{p}_{N_T}} & \frac{\partial \ln f(z_2^C|\boldsymbol{p}_{N_T})}{\partial \boldsymbol{p}_{N_T}} & \cdots & \frac{\partial \ln f(z_{N_T}^C|\boldsymbol{p}_{N_T})}{\partial \boldsymbol{p}_{N_T}} \end{pmatrix} = \begin{pmatrix} \frac{\partial \ln f(z_1^C|\boldsymbol{p}_1)}{\partial \boldsymbol{p}_1} & \frac{\partial \ln f(z_{1,2}|\boldsymbol{p}_1)}{\partial \boldsymbol{p}_1} & \cdots & \frac{\partial \ln f(z_{1,N_T}|\boldsymbol{p}_1)}{\partial \boldsymbol{p}_1} \\ \frac{\partial \ln f(z_{2,1}|\boldsymbol{p}_2)}{\partial \boldsymbol{p}_2} & \frac{\partial \ln f(z_2^C|\boldsymbol{p}_2)}{\partial \boldsymbol{p}_2} & \cdots & \frac{\partial \ln f(z_{2,N_T}|\boldsymbol{p}_2)}{\partial \boldsymbol{p}_2} \\ \vdots & \vdots & \ddots & \vdots \\ \frac{\partial \ln f(z_{N_T,1}|\boldsymbol{p}_{N_T})}{\partial \boldsymbol{p}_{N_T}} & \frac{\partial \ln f(z_{N_T,2}|\boldsymbol{p}_{N_T})}{\partial \boldsymbol{p}_{N_T}} & \cdots & \frac{\partial \ln f(z_{N_T}^C|\boldsymbol{p}_{N_T})}{\partial \boldsymbol{p}_{N_T}} \end{pmatrix} \tag{49}$$

$$\mathbf{D}_C = \boldsymbol{x}^T \mathbf{G}_C^T \left( \sum_{i=1}^{N_T} \Gamma_i \right) \mathbf{G}_C \boldsymbol{x} + \boldsymbol{x}^T \mathbf{G}_C^T \Xi \mathbf{G}_C \boldsymbol{x} = \boldsymbol{x}^T \mathbf{G}_C^T \left( \sum_{i=1}^{N_T} \Gamma_i + \Xi \right) \mathbf{G}_C \boldsymbol{x} \tag{59}$$

$$\Gamma_i = \mathrm{diag}\left(\frac{\xi_{1,i}\beta^2(\frac{f_c}{4\pi})^{2\beta}}{d_{1,i}^{2\beta+2}N_0}, \ldots, \frac{\xi_{i-1,i}\beta^2(\frac{f_c}{4\pi})^{2\beta}}{d_{i-1,i}^{2\beta+2}N_0}, 0, \frac{\xi_{i+1,i}\beta^2(\frac{f_c}{4\pi})^{2\beta}}{d_{i+1,i}^{2\beta+2}N_0}, \ldots, \frac{\xi_{N_T,i}\beta^2(\frac{f_c}{4\pi})^{2\beta}}{d_{N_T,i}^{2\beta+2}N_0}\right) \tag{60}$$

where $\mathbf{U}_\psi$ is the eigenvector matrix and $\tau_1, \ldots, \tau_{N_T}$ are the corresponding eigenvalues. Then, $\mathrm{tr}\{\mathbf{J}(\boldsymbol{\theta})\} = \sum_{i=1}^{2N_T} \tau_i$ and $\mathcal{P}(\boldsymbol{\theta}) = \sum_{i=1}^{2N_T} (1/\tau_i)$. Considering each eigenvalue is positive in FIM, we attain the following formulation according to [47]:

$$\frac{2N_T}{\sum_{i=1}^{2N_T} \frac{1}{\tau_i}} \leq \frac{1}{2N_T} \sum_{i=1}^{2N_T} \tau_i. \tag{55}$$

Then, we obtain $\mathcal{P}(\boldsymbol{\theta}) \geq 4N_T^2(1/[\mathrm{tr}\{\mathbf{J}(\boldsymbol{\theta})\}])$.

For $\mathbf{J}(\boldsymbol{\theta})$

$$\begin{aligned} \mathrm{tr}\{\mathbf{J}(\boldsymbol{\theta})\} &= \mathrm{tr}\left( \sum_{i=1}^{N_T} \mathbf{J}_A(\boldsymbol{p}_i) + \sum_{i=1}^{N_T} \sum_{m \neq i}^{N_T} \mathbf{C}_{m,i} \right) \\ &= \sum_{i=1}^{N_T} \sum_{j=1}^{N_A} \lambda_{j,i} + \sum_{i=1}^{N_T} \sum_{m \neq i}^{N_T} \left( \lambda_{i,m} + \lambda_{m,i} \right) \\ &= \mathbf{D}_A + \mathbf{D}_C \end{aligned} \tag{56}$$

Substituting (47) into $\mathbf{D}_A$, we attain

$$\mathbf{D}_A = \boldsymbol{x}^T \mathbf{G}_A^T \sum_{i=1}^{N_T} \Lambda_i \mathbf{G}_A \boldsymbol{x} \tag{57}$$

where $\Lambda_i = \mathrm{diag}([(\xi_{1,i}\beta^2(f_c/4\pi)^{2\beta})/(d_{1,i}^{2\beta+2}N_0)] \ , \ldots, [(\xi_{N_A,i}\beta^2(f_c/4\pi)^{2\beta})/d_{N_A,i}^{2\beta+2}N_0])$. Then, we substitute (53) into $\mathbf{D}_C$ and divide $\mathbf{D}_C = \sum_{i=1}^{N_T} \sum_{m \neq i}^{N_T} \lambda_{i,m} + \sum_{i=1}^{N_T} \sum_{m \neq i}^{N_T} \lambda_{m,i}$ to attain (59), shown at the top of the page, where $\Gamma_i$ is formulated as (60), shown at the top of the page and $\Xi$ is expressed as

$$\Xi = \mathrm{diag}\left( \sum_{m \neq 1}^{N_T} \frac{\xi_{1,m}\beta^2\left(\frac{f_c}{4\pi}\right)^{2\beta}}{d_{1,m}^{2\beta+2}N_0}, \ldots, \sum_{m \neq N_T}^{N_T} \frac{\xi_{N_T,m}\beta^2\left(\frac{f_c}{4\pi}\right)^{2\beta}}{d_{N_T,m}^{2\beta+2}N_0} \right). \tag{58}$$

## REFERENCES


[1] J. Huang, Y. Zhou, Z. Ning, and H. Gharavi, "Wireless power transfer and energy harvesting: Current status and future prospects," *IEEE Wireless Commun.*, vol. 26, no. 4, pp. 163–169, Aug. 2019.

[2] R. Bansal, "The future of wireless charging [AP-S Turnstile]," *IEEE Antennas Propag. Mag.*, vol. 51, no. 2, p. 153, Apr. 2009.

[3] Y. Shen and M. Z. Win, "Fundamental limits of wideband localization—Part I: A general framework," *IEEE Trans. Inf. Theory*, vol. 56, no. 10, pp. 4956–4980, Oct. 2010.

[4] K. W. Choi *et al.*, "Toward realization of long-range wireless-powered sensor networks," *IEEE Wireless Commun.*, vol. 26, no. 4, pp. 184–192, Aug. 2019.

[5] P. Biswas, T.-C. Lian, T.-C. Wang, and Y. Ye, "Semidefinite programming based algorithms for sensor network localization," *ACM Trans. Sens. Netw.*, vol. 2, no. 2, pp. 188–220, 2006.

[6] G. Yang, C. K. Ho, R. Zhang, and Y. L. Guan, "Throughput optimization for massive MIMO systems powered by wireless energy transfer," *IEEE J. Sel. Areas Commun.*, vol. 33, no. 8, pp. 1640–1650, Aug. 2015.

[7] F. Tan, T. Lv, and P. Huang, "Global energy efficiency optimization for wireless-powered massive MIMO aided multiway AF relay networks," *IEEE Trans. Signal Process.*, vol. 66, no. 9, pp. 2384–2398, May 2018.

[8] Y. Kim, T.-J. Lee, and D. I. Kim, "Joint information and power transfer in SWIPT-enabled CRFID networks," *IEEE Wireless Commun. Lett.*, vol. 7, no. 2, pp. 186–189, Apr. 2018.

[9] G. Loubet, A. Takacs, and D. Dragomirescu, "Implementation of a battery-free wireless sensor for cyber-physical systems dedicated to structural health monitoring applications," *IEEE Access*, vol. 7, pp. 24679–24690, 2019.

[10] W. Feng *et al.*, "Joint 3D trajectory design and time allocation for UAV-enabled wireless power transfer networks," *IEEE Trans. Veh. Technol.*, vol. 69, no. 9, pp. 9265–9278, Sep. 2020.
[11] J. Rezazadeh, R. Subramanian, K. Sandrasegaran, X. Kong, M. Moradi, and F. Khodamoradi, "Novel iBeacon placement for indoor positioning in IoT," *IEEE Sensors J.*, vol. 18, no. 24, pp. 10240–10247, Dec. 2018.
[12] W. Dai, Y. Shen, and M. Z. Win, "Distributed power allocation for cooperative wireless network localization," *IEEE J. Sel. Areas Commun.*, vol. 33, no. 1, pp. 28–40, Jan. 2015.
[13] Y. Shen, W. Dai, and M. Z. Win, "Power optimization for network localization," *IEEE/ACM Trans. Netw.*, vol. 22, no. 4, pp. 1337–1350, Aug. 2014.
[14] W. W. Li, Y. Shen, Y. J. Zhang, and M. Z. Win, "Robust power allocation for energy-efficient location-aware networks," *IEEE/ACM Trans. Netw.*, vol. 21, no. 6, pp. 1918–1930, Dec. 2013.
[15] H. Ju and R. Zhang, "Throughput maximization in wireless powered communication networks," *IEEE Trans. Wireless Commun.*, vol. 13, no. 1, pp. 418–428, Jan. 2014.
[16] Y. L. Che, L. Duan, and R. Zhang, "Spatial throughput maximization of wireless powered communication networks," *IEEE J. Sel. Areas Commun.*, vol. 33, no. 8, pp. 1534–1548, Aug. 2015.
[17] N. K. D. Venkategowda, H. Lee, and I. Lee, "Joint transceiver designs for MSE minimization in MIMO wireless powered sensor networks," *IEEE Trans. Wireless Commun.*, vol. 17, no. 8, pp. 5120–5131, Aug. 2018.
[18] Z. Zhou, M. Peng, and Z. Zhao, "Joint data-energy beamforming and traffic offloading in cloud radio access networks with energy harvesting-aided D2D communications," *IEEE Trans. Wireless Commun.*, vol. 17, no. 12, pp. 8094–8107, Dec. 2018.
[19] H. Wang, J. Wang, G. Ding, and Z. Han, "D2D communications underlaying wireless powered communication networks," *IEEE Trans. Veh. Technol.*, vol. 67, no. 8, pp. 7872–7876, Aug. 2018.
[20] K. Liang, L. Zhao, G. Zheng, and H. H. Chen, "Non-uniform deployment of power beacons in wireless powered communication networks," *IEEE Trans. Wireless Commun.*, vol. 18, no. 3, pp. 1887–1899, Mar. 2019.
[21] T. Ha, J. Kim, and J.-M. Chung, "HE-MAC: Harvest-then-transmit based modified EDCF MAC protocol for wireless powered sensor networks," *IEEE Trans. Wireless Commun.*, vol. 17, no. 1, pp. 3–16, Jan. 2018.
[22] J. Chen, L. Zhang, Y.-C. Liang, X. Kang, and R. Zhang, "Resource allocation for wireless-powered IoT networks with short packet communication," *IEEE Trans. Wireless Commun.*, vol. 18, no. 2, pp. 1447–1461, Feb. 2019.
[23] Y. Qian *et al.*, "Design of hybrid wireless and power line sensor networks with dual-interface relay in IoT," *IEEE Internet Things J.*, vol. 6, no. 1, pp. 239–249, Feb. 2019.
[24] T. V. Nguyen, T.-N. Do, V. N. Q. Bao, D. B. d. Costa, and B. An, "On the performance of multihop cognitive wireless powered D2D communications in WSNs," *IEEE Trans. Veh. Technol.*, vol. 69, no. 3, pp. 2684–2699, Mar. 2020.
[25] W. Wang *et al.*, "Joint precoding optimization for secure SWIPT in UAV-aided NOMA networks," *IEEE Trans. Commun.*, vol. 68, no. 8, pp. 5028–5040, Aug. 2020.
[26] M. R. Basheer and S. Jagannathan, "Localization of RFID tags using stochastic tunneling," *IEEE Trans. Mobile Comput.*, vol. 12, no. 6, pp. 1225–1235, Jun. 2013.
[27] R. Vauche, E. Bergeret, J. Gaubert, S. Bourdel, O. Fourquin, and N. Dehaese, "A remotely UHF powered UWB transmitter for high precision localization of RFID tag," in *Proc. IEEE Int. Conf. Ultra-Wideband (ICUWB)*. 2011, pp. 494–498.
[28] P. Pannuto, B. Kempke, and P. Dutta, "Slocalization: Sub-uW ultra wideband backscatter localization," in *Proc. 17th ACM/IEEE Int. Conf. Inf. Process. Sens. Netw. (IPSN)*, 2018, pp. 242–253.
[29] M. Fantuzzi, D. Masotti, and A. Costanzo, "Rectenna array with RF-uncoupled closely-spaced monopoles for autonomous localization," in *Proc. 48th Eur. Microw. Conf. (EuMC)*, 2018, pp. 765–768.
[30] M. Fantuzzi, D. Masotti, and A. Costanzo, "A multilayer compact-size UWB-UHF antenna system for novel RFID applications," in *Proc. Eur. Microw. Conf. (EuMC)*, 2015, pp. 255–258.
[31] M. Fantuzzi, D. Masotti, and A. Costanzo, "A novel integrated UWB–UHF one-port antenna for localization and energy harvesting," *IEEE Trans. Antennas Propag.*, vol. 63, no. 9, pp. 3839–3848, Sep. 2015.
[32] A. El Assaf, S. Zaidi, S. Affes, and N. Kandil, "Efficient node localization in energy-harvesting wireless sensor networks," in *Proc. IEEE Int. Conf. Ubiquitous Wireless Broadband (ICUWB)*, 2015, pp. 1–7.
[33] Z. Chang, X. Wu, W. Wang, and G. Chen, "Localization in wireless rechargeable sensor networks using mobile directional charger," in *Proc. IEEE Global Commun. Conf. (GLOBECOM)*, 2015, pp. 1–6.
[34] D. Belo, D. C. Ribeiro, P. Pinho, and N. B. Carvalho, "A selective, tracking, and power adaptive far-field wireless power transfer system," *IEEE Trans. Microw. Theory Techn.*, vol. 67, no. 9, pp. 3856–3866, Sep. 2019.
[35] A. A. Aziz *et al.*, "Battery-less location tracking for Internet of Things: Simultaneous wireless power transfer and positioning," *IEEE Internet Things J.*, vol. 6, no. 5, pp. 9147–9164, Oct. 2019.
[36] Y. Zhao, X. Li, Y. Ji, and C.-Z. Xu, "Wireless power-driven positioning system: Fundamental analysis and resource allocation," *IEEE Internet Things J.*, vol. 6, no. 6, pp. 10421–10430, Dec. 2019.
[37] M. Z. Win, R. M. Buehrer, G. Chrisikos, A. Conti, and H. V. Poor, "Foundations and trends in localization technologies: Part I [scanning the issue]," *Proc. IEEE*, vol. 106, no. 6, pp. 1019–1021, Jun. 2018.
[38] Y. Shen, H. Wymeersch, and M. Z. Win, "Fundamental limits of wideband localization—Part II: Cooperative networks," *IEEE Trans. Inf. Theory*, vol. 56, no. 10, pp. 4981–5000, Oct. 2010.
[39] W. Dai, Y. Shen, and M. Z. Win, "Energy-efficient network navigation algorithms," *IEEE J. Sel. Areas Commun.*, vol. 33, no. 7, pp. 1418–1430, Jul. 2015.
[40] T. Zhang, A. F. Molisch, Y. Shen, Q. Zhang, H. Feng, and M. Z. Win, "Joint power and bandwidth allocation in wireless cooperative localization networks," *IEEE Trans. Wireless Commun.*, vol. 15, no. 10, pp. 6527–6540, Oct. 2016.
[41] J. Chen, W. Dai, Y. Shen, V. K. N. Lau, and M. Z. Win, "Resource management games for distributed network localization," *IEEE J. Sel. Areas Commun.*, vol. 35, no. 2, pp. 317–329, Feb. 2017.
[42] B. Peng, G. Seco-Granados, E. Steinmetz, M. Fröhle, and H. Wymeersch, "Decentralized scheduling for cooperative localization with deep reinforcement learning," *IEEE Trans. Veh. Technol.*, vol. 68, no. 5, pp. 4295–4305, May 2019.
[43] S. Safavi, U. A. Khan, S. Kar, and J. M. F. Moura, "Distributed localization: A linear theory," *Proc. IEEE*, vol. 106, no. 7, pp. 1204–1223, Jul. 2018.
[44] T. V. Nguyen, Y. Jeong, H. Shin, and M. Z. Win, "Least square cooperative localization," *IEEE Trans. Veh. Technol.*, vol. 64, no. 4, pp. 1318–1330, Apr. 2015.
[45] R. M. Vaghefi and R. M. Buehrer, "Cooperative localization in NLOS environments using semidefinite programming," *IEEE Commun. Lett.*, vol. 19, no. 8, pp. 1382–1385, Aug. 2015.
[46] S. M. Kay, *Fundamentals of Statistical Signal Processing: Estimation Theory*. Englewood Cliffs, NJ, USA: Prentice Hall PTR, 1993.
[47] L. Rabinowitz, "Mathematical statistics and data analysis," *Technometrics*, vol. 31, no. 3, pp. 390–391, 1989.

**Yubin Zhao** (Member, IEEE) received the B.S. and M.S. degrees from Beijing University of Posts and Telecommunications, Beijing, China, in 2007 and 2010, respectively, and the Ph.D degree in computer science from the Freie Universität Berlin, Berlin, Germany, in 2014.

He has been an Associate Professor with the Center for Cloud Computing, Shenzhen Institutes of Advanced Technology, Chinese Academy of Sciences, Shenzhen, China, since 2014. He is currently an Associate Professor with the School of Microelectronics Science and Technology, Sun Yat-Sen University, Guangzhou, China. His current research interest includes wireless power transfer, indoor localization and target tracking.

Dr. Zhao received the Outstanding Research Award in CICCAT 2019. He serves as the guest editor and a reviewer for several journals.

**Xiaofan Li** (Senior Member, IEEE) received the B.S. and Ph.D. degrees from Beijing University of Posts and Telecommunication, Beijing, China, in 2007 and 2012, respectively.

From 2010 to 2011, she studied with the University of Washington as an exchanged Ph.D student. She joined the State Radio Monitoring Center and Testing Center (SRTC), Beijing, in 2012. He was transferred to SRTC Shenzhen Laboratory, Shenzhen, in 2013. She is currently an Associate Professor with the School of Intelligent Systems Science and Engineering, Jinan University, Zhuhai, China. Her research interests include interference analysis among different radio systems, testing and evaluation methods for innovative radio technologies, cooperative communication, cognitive radio, Internet of Things, and radio management strategy.

**Huaming Wu** (Member, IEEE) received the B.E. and M.S. degrees in electrical engineering from Harbin Institute of Technology, Harbin, China, in 2009 and 2011, respectively, and the Ph.D. degree (Highest Hons.) in computer science from the Freie Universität Berlin, Berlin, Germany, in 2015.

He is currently an Associate Professor with the Center for Applied Mathematics, Tianjin University, Tianjin, China. His research interests include model-based evaluation, wireless and mobile network systems, mobile cloud computing, and deep learning.

**Cheng-Zhong Xu** (Fellow, IEEE) received the B.Sc. and M.Sc. degrees in computer science and engineering from Nanjing University, Nanjing, China, in 1986 and 1989, respectively, and the Ph.D. degree in computer science and engineering from the University of Hong Kong, Hong Kong, in 1993.

He is the Dean of the Faculty of Science and Technology, University of Macau, Macau, China, where he is a Chair Professor of Computer and Information Science and the Interim Director of Institute of Collaborative Innovation. He also holds a courtesy position as the Director of the Center for Cloud Computing, Shenzhen Institutes of Advanced Technology (SIAT), Chinese Academy of Sciences, Shenzhen, China. He was a Professor of Electrical and Computer Engineering with Wayne State University, Detroit, MI, USA, and the Director of Advanced Computing and Digital Engineering, SIAT. He published two research monographs and more than 250 papers in journals and conference proceedings, including over 50 in IEEE/ACM transactions; his publications received more than 9000 citations with an H-index of 47. His main research interests lie in parallel and distributed computing and cloud computing, in particular, with an emphasis on resource management for system's performance, reliability, availability, power efficiency, and security, and in big data and data-driven intelligence applications. The systems of particular interests include distributed systems and the Internet, servers and cloud datacenters, scalable parallel computers, and wireless-embedded devices, and mobile-edge systems.

Dr. Xu was a Best Paper Nominee or Awardee of the 2013 IEEE High Performance Computer Architecture (HPCA) and the 2013 ACM High Performance Distributed Computing, IEEE Cluster2015, ICPP2015, GPC2018, and UIC2018. He received the most prestigious President's Awards for Excellence in Teaching of Wayne State University in 2002. He also received more than 100 patents or PCT patents and spun off a business Shenzhen Baidou Applied Technology with dedication to location-based services and technologies. He serves or served on a number of journal editorial boards, including IEEE TRANSACTIONS ON COMPUTERS, IEEE TRANSACTIONS ON CLOUD COMPUTING, IEEE TRANSACTIONS ON PARALLEL AND DISTRIBUTED SYSTEMS, *Journal of Parallel and Distributed Computing*, *Science China: Information Science*, and *ZTE Communication*. He has been the Chair of IEEE Technical Committee on Distributed Processing since 2015.